Eur Respir J 2003; 22: 227–234
DOI: 10.1183/09031936.03.00064203
Printed in UK – all rights reserved

European Respiratory Journal
ISSN 0903-1936

Mechanics and crossbridge kinetics of tracheal smooth muscle in two inbred rat strains

F-X. Blanc*,#, C. Coirault*,¶, S. Salmeron*,#, D. Chemla*,¶, Y. Lecarpentier*,¶

Mechanics and crossbridge kinetics of tracheal smooth muscle in two inbred rat strains. F-X. Blanc, C. Coirault, S. Salmeron, D. Chemla, Y. Lecarpentier. ©ERS Journals Ltd 2003.

ABSTRACT: The aim of the study was to determine whether the nonspecific *in vivo* airway hyperresponsiveness of the inbred Fisher F-344 rat strain was associated with differences in the intrinsic contractile properties of tracheal smooth muscle (TSM) when compared with Lewis rats.

Isotonic and isometric contractile properties of isolated TSM from Fisher and Lewis rats (each n=10) were investigated, and myosin crossbridge (CB) number, force and kinetics in both strains were calculated using Huxley's equations adapted to nonsarcomeric muscles. Maximum unloaded shortening velocity and maximum extent of muscle shortening were higher in Fisher than in Lewis rats (~46% and ~42%, respectively), whereas peak isometric tension was similar.

The curvature of the hyperbolic force/velocity relationship did not differ between strains. Myosin CB number and unitary force were similar in both strains. The duration of CB detachment and attachment was shorter in Fisher than in Lewis rats (~-46% and -34%, respectively).

In Fisher rats, these results show that inherited, genetically determined factors of airway hyperresponsiveness are associated with changes in crossbridge kinetics, contributing to an increased tracheal smooth muscle shortening capacity and velocity. *Eur Respir J 2003; 22: 227–234.*

*INSERM LOA ENSTA, Polytechnic School, Palaiseau, #Pneumology Unit, Dept of Internal Medicine, and ¶Dept of Cardiovascular and Respiratory Physiology, Bicêtre Hospital, University of Paris XI, Assistance Publique, Hôpitaux de Paris, Le Kremlin-Bicêtre, France.

Correspondence: F-X. Blanc, Unité de Pneumologie, Service de Médecine Interne, Centre Hospitalier Universitaire de Bicêtre, 78, rue du Général Leclerc, 94275 Le Kremlin-Bicêtre, France.
Fax: 33 145212632
E-mail: xavier.blanc@bct.ap-hop-paris.fr

Keywords: Airways, crossbridge, hyperresponsiveness, myosin, smooth muscle

Received: July 17 2002
Accepted after revision: March 25 2003

S. Salmeron was the recipient of a grant from CNRS and AP-HP (Praticien de Recherche Associé).

Asthma is characterised by chronic inflammatory disorders of the airways associated with increased airway responsiveness to various stimuli [1]. The mechanisms underlying nonspecific airway hyperresponsiveness (AHR) remain poorly understood. Although it is clear that airway smooth muscle (ASM) is the key effector of excessive airway narrowing in asthma, it remains unclear whether or not AHR is attributable to ASM abnormality [2, 3]. The amount of ASM has been reported to be increased in human asthmatics [4–6] and in animal models of AHR [7]. However, recent stereological studies using axial airway sections at high resolution have provided no evidence of increased ASM in large airways of human asthmatics [8]. Marked differences in isotonic contractile properties of isolated ASM have been reported in human asthmatic [9], and in human- [10] and animal-sensitised [11–14] tissues. In these studies, isolated ASM was found to shorten more and faster in asthmatic and sensitised tissues than in controls without any differences in the ability to generate force. Taken together, these findings suggest functional changes resulting in increased ASM shortening capacity and velocity in hyperresponsive airways, without increases in the amount of ASM [8] or in ASM force production capacity. Potential mechanisms involved in such an increased ASM shortening capacity and velocity include reduced bronchial stiffness [9], decreased resistance to internal shortening [15], and increased myosin crossbridge (CB) cycling rate possibly related to an increased content of smooth-muscle myosin light-chain kinase (smMLCK) [16].

To study the direct contribution of ASM in the phenomenon of AHR, two complementary approaches are generally used in animals. First, various models dealing with passive or active sensitisation are used to investigate the acquired mechanisms involved in AHR. Second, models of spontaneous, nonspecific AHR can be used to study the inherited, genetically determined factors associated with AHR. To the best of the authors' knowledge, ASM isotonic mechanical properties have never been studied in animal models of spontaneous genetically determined AHR. Two rat strains have been studied extensively because of marked differences in their spontaneous airway responsiveness, the Fisher F-344 strain and the Lewis strain. When compared with the Lewis strain, the Fisher strain exhibited greater airway responsiveness to various inhaled contractile agonists, such as methacholine [17] and 5-hydroxytryptamine [18, 19]. This relative AHR was manifested by a shift in the dose/response curve to the aerosolised agonist in both spontaneously breathing [17–19] and mechanically ventilated animals [20].

The aim of the present study was to determine whether the nonspecific *in vivo* AHR of the Fisher F-344 rat strain was associated with differences in the intrinsic contractile properties of tracheal smooth muscle (TSM) when compared with Lewis rats. Therefore, the mechanical properties of isolated TSM of inbred Fisher and Lewis rats were studied, focusing on isotonic parameters (extent and velocity of shortening), and the hypothesis of whether potential, inherited, genetically

determined mechanical differences could be attributed to differences in myosin CB interactions was tested.

Materials and methods

Tracheal smooth muscle preparation

Experiments were conducted with highly inbred male rats obtained from Charles River (Sulzfeld, Germany). Care of animals conformed to the recommendations of the Helsinki convention and the study was approved by the authors' institution (INSERM, France). Ten adult Fisher F-344 rats (means±SEM weight 208±12 g) and 10 adult Lewis rats (weight 215±14 g; p=0.71) were studied after being housed at a conventional animal facility where all animals had free access to food and water. At the time of the experiment, the investigator was not aware of which strain was Fisher or Lewis. For each animal, experiments were performed on TSM obtained from a tracheal ring consisting of four segments. The ring was opened with a dorsal midline section through the cartilage in order to obtain a strip of the posterior membranous portion of the trachea. The epithelium was not removed. The strip was then vertically suspended in a 100 mL organ bath containing a Krebs-Henseleit solution, bubbled with 95% oxygen/5% carbon dioxide and maintained at 37°C, pH 7.4. The lower end of the strip was held by a stationary clip at the bottom of the bath, while the upper extremity was held in a spring clip linked to an electromagnetic lever system [21, 22]. Supramaximal electrical field stimulation (EFS; 30 $V \cdot cm^{-1}$, 50 Hz AC, 3 ms pulse duration, 12 s train duration) was applied every 4 min by means of two platinum electrodes arranged in parallel on either side of the muscle preparation. Mechanical experiments were conducted after a 1-h equilibration period.

Mechanical parameters, force/velocity relationship

Mechanical parameters were recorded at optimal initial muscle length (L_0) over the load continuum [21, 22]. According to the conventional afterloaded technique, 8–10 EFS-elicited contractions were performed against increasing loads, from zero-load up to the fully isometric contraction. Maximum unloaded shortening velocity (V_{max}; $L_0 \cdot s^{-1}$), using the zero-load clamp technique [23], maximum shortening velocity at the preload required to obtain L_0 ($V_{c,max}$; $L_0 \cdot s^{-1}$) and maximum extent of shortening at preload (ΔL; $\%L_0$) were measured. Peak isometric force (F_0; mN) was also measured and normalised per cross-sectional area to obtain peak isometric tension (P_0; $mN \cdot mm^{-2}$). For each contraction, peak shortening velocity (V) was plotted against total isotonic load normalised per cross-sectional area (P). Data from the force/velocity curve were fitted according to HILL's [24] hyperbolic equation, -a and -b being the asymptotes of the hyperbola, and G being the curvature of the hyperbola. At the end of the study, cross-sectional area (mm^2) was calculated from the ratio of muscle weight (mg) to muscle length at L_0 (mm), assuming a muscle density of 1 [25]. Mean cross-sectional area did not differ between groups (1.17±0.12 mm^2 in Fisher *versus* 0.94±0.08 mm^2 in Lewis, p=0.12).

Calculation of myosin crossbridge number, force and kinetics

HUXLEY's [26] original equations constitute the most widely accepted mathematical model of muscle contraction. This model provides an informative system for estimating the number, unitary force and kinetics of myosin CB in living striated muscles. An adaptation of these equations to nonsarcomeric muscles, such as smooth muscles, was recently developed [27]. This approach allows calculation of the unitary force per CB (Π_0; pN), the number of CB per mm^2 at peak active tension ($\Psi \times 10^9$), mean CB velocity during power stroke (v_0; $\mu m \cdot s^{-1}$), total duration of the CB cycle (t_c; ms), the rate of adenosine triphosphatase (ATPase) activity (k_{cat}, with $k_{cat}=1/t_c$) and duration of CB attachment ($1/f_1$; ms) and detachment ($1/g_2$; ms), where f_1 represents peak value of attachment rate constant and g_2 represents peak value of detachment rate constant (another constant of detachment being termed g_1; fig. 1).

In fact, if h is termed the molecular step size (h=11 nm in ASM) [28, 29], it can be seen from HUXLEY's [26] manuscript, that $\phi=(f_1+g_1)h/2$ and that it is assumed that $\phi=b$ and $G=g_2/(f_1+g_1)$. If w is termed the mechanical work of a single CB ($w=3.8\times10^{-20}$ J) [26, 30], e is termed the free energy required to split one adenosine triphosphate (ATP) molecule ($e=5.1\times10^{-20}$ J) [26, 30], and l is termed the length between two actin binding sites (l=36 nm) [31], then the following is obtained:

$$g_1 = 2wb/ehG \quad (1)$$

$$g_2 = 2V_{max}/h \quad (2)$$

$$f_1 = \frac{-g_1 + \sqrt{g_a^2 + 4g_1g_2}}{2} \quad (3)$$

$$\Pi_0 = \frac{w}{l} \times \frac{f_1}{f_1 + g_1} \quad (4)$$

$$\Psi = ab/\left(e\frac{h}{2\ell} \times \frac{f_1 g_1}{f_1 + g_1}\right) \quad (5)$$

$$v_0 = ab/\Psi\Pi_0 L_0 \quad (6)$$

$$t_c = 1/\frac{h}{2\ell} \times \frac{f_1 g_1}{f_1 + g_1} \quad (7)$$

For each TSM, the number, force and kinetics of CB were calculated by substituting the measured values of the force/velocity relationship (namely V_{max}, a, b, G) in the seven

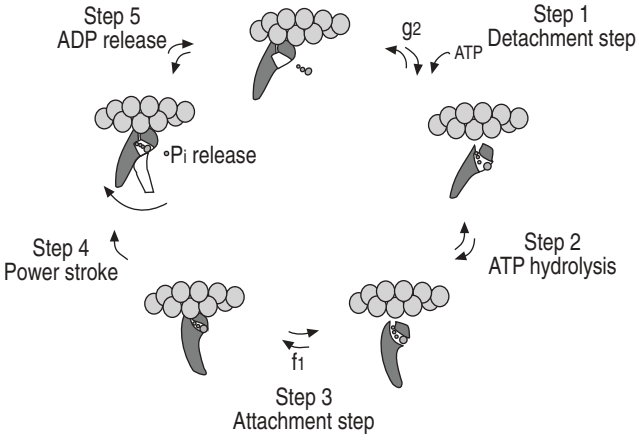

Fig. 1. – Schematic representation of the crossbridge cycle. The power stroke (*i.e.* the displacement of the myosin head and the force generation) is triggered by the release of the inorganic phosphate (P_i; step 4) and occurs after adenosine triphosphate (ATP) hydrolysis (step 2) and attachment of the myosin head to the actin filament (step 3). Myosin rapidly dissociates from actin (step 1) after adenosine diphosphate (ADP) release (step 5). g_2: peak value of detachment rate constant; f_1: peak value of attachment rate constant.

above-mentioned equations (for details see Appendix [26, 27, 32]).

Statistical analysis

All data are expressed as mean±SEM. Statistical comparisons between groups were carried out by using an unpaired t-test. For the force/velocity curves, a correlation coefficient (r) between measured values of force and velocity and the model estimate was used to test the accuracy of the hyperbolic fit. The correlation between two variables was calculated by linear regression using the least-squares method. A $p<0.05$ was considered statistically significant.

Results

Classic mechanical parameters in tracheal smooth muscle of rats

During the EFS elicited after loaded contractions, peak isometric force was higher in Fisher than in Lewis rats (fig. 2). However, when normalised by cross-sectional area, peak isometric tension (P0) did not differ between Fisher and Lewis rats: P0 was 16.16±2.01 $mN \cdot mm^{-2}$ in Fisher and 15.10± 1.92 $mN \cdot mm^{-2}$ in Lewis rats (p=0.71). Compared with Lewis rats, Fisher rats exhibited faster Vmax (~46%, p<0.001; fig. 2), faster Vc,max (~63%, p<0.05; fig. 3) and a greater ΔL (~42%, p<0.05; fig. 3).

Force/velocity relationship of tracheal smooth muscle in rats

In both strains, the force/velocity relationship was accurately fitted by a hyperbola: the r value between experimental data and Hill′s model was 0.993±0.001 and 0.997±0.001 in Fisher and Lewis rats, respectively. As shown in table 1, parameter b (which has units of velocity) was higher in Fisher than in Lewis rats. Conversely, parameter a (which has units of tension) was similar in both strains, as was the G curvature of the hyperbolic force/velocity relationship (table 1). Figure 4 shows representative force per mm^2/velocity curves in Fisher and Lewis TSM.

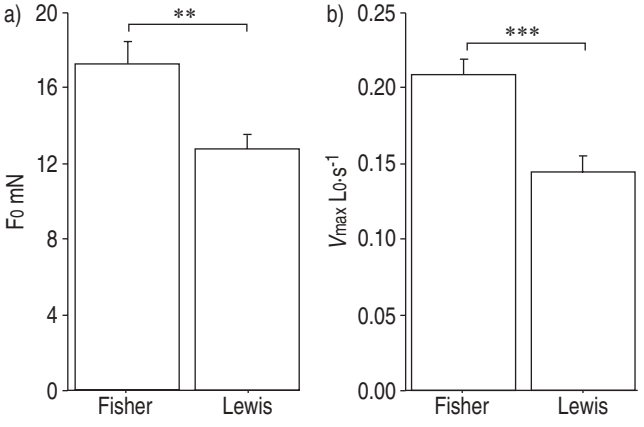

Fig. 2. – Mean±SEM a) peak isometric force (F0) and b) maximum unloaded shortening velocity (Vmax) measured in Fisher (n=10) and Lewis (n=10) rats. **: p<0.01; ***: p<0.001.

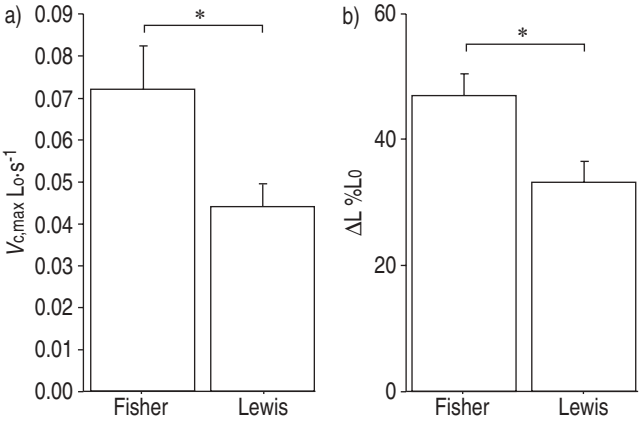

Fig. 3. – Mean±SEM isotonic mechanical parameters measured at preload in Fisher (n=10) and Lewis (n=10) rats. a) Maximum shortening velocity of tracheal smooth muscle (Vc,max) and b) maximum extent of shortening (ΔL). L0: optimal initial muscle length. *: p<0.05.

Table 1. – Constants derived from the Hill equation in force/velocity curves elicited with afterloaded contractions in Fisher and Lewis rats

	Fisher	Lewis
-a $mN \cdot mm^{-2}$	-4.3±0.5	4.8±0.6
-b $L0 \cdot s^{-1}$	-0.063±0.005	0.047±0.004*
G	3.9±0.5	3.3±0.3

Data are presented as mean±SEM. L0: optimal initial muscle length; -a and -b: the asymptotes of the hyperbola; G: the curvature of the hyperbola. n=10 for both. *: p<0.05.

Myosin crossbridge number, force and kinetics

Π0 and the number of CB at peak active tension (Ψ× 10^9) are depicted in figure 5. No significant differences were observed between Fisher and Lewis rats. There were no strain differences in mean CB velocity during power stroke (v0=0.249±0.040 $\mu m \cdot s^{-1}$ in Fisher and v0=0.246±0.046 $\mu m \cdot s^{-1}$ in Lewis rats, p=0.95). There was no correlation between the Vmax and v0 (r^2=0.056, p=0.32). There was a weak correlation between P0 of the muscle strip and Π0 (r^2=0.223, p<0.05; fig. 6a). Figure 6b shows that there was a strong linear relationship between P0 of the muscle strip and Ψ.

Myosin CB kinetics are depicted in figure 7; the duration of both 1/g2 and 1/f1 was significantly shorter in Fisher than in Lewis rats (-46% and -34%, respectively). The tc did not differ between strains: tc was 4.354±0.815 s in Fisher and 4.819± 0.590 s in Lewis rats (p=0.65). kcat did not differ between strains: kcat was 0.301±0.046·s^{-1} in Fisher and 0.242±0.036·s^{-1} in Lewis (p=0.33).

Discussion

The major findings of the present study are that: 1) the higher genetically determined spontaneous nonspecific AHR of the Fisher rat strain is associated with higher shortening capacity and velocity of isolated TSM when compared with Lewis; 2) myosin CB kinetics differ between strains; 1/g2 and, to a lesser extent, 1/f1 is shorter in Fisher than in Lewis rats, and 3) P0 and the unitary force per CB were similar in both strains, although F0 was higher in Fisher than in Lewis rats.

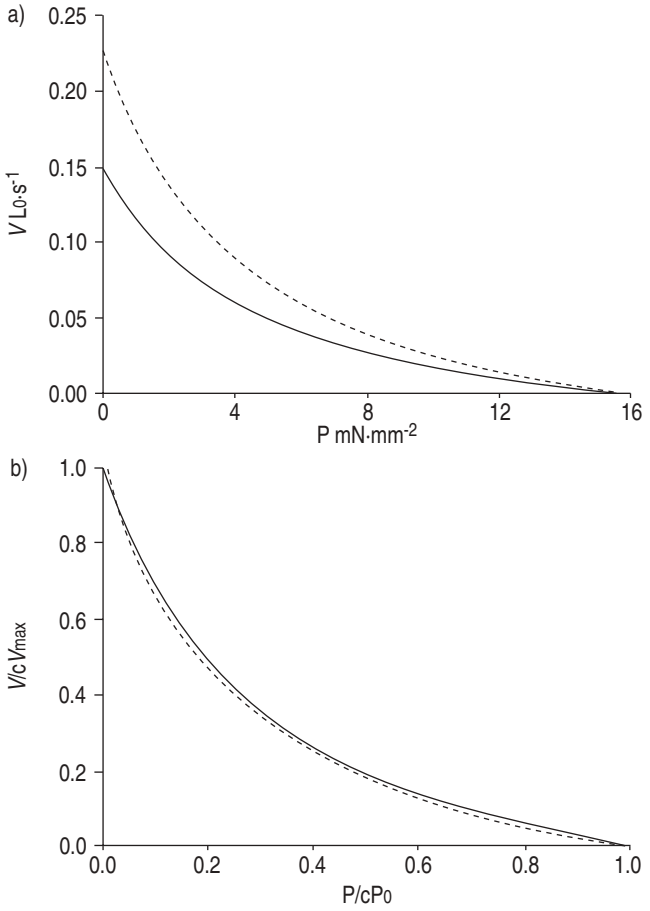

Fig. 4. – Representative force per mm^2 (P)/velocity (V) curves for Fisher (- - -) and Lewis (——) rat tracheal smooth muscle. a) Absolute P and V values were used to determine the P/V relationships. b) Normalised P and V values were used to determine the G curvature of the hyperbola. L_0: optimal initial muscle length; cV_{max}: calculated maximum shortening velocity; cP_0: calculated maximum isometric tension.

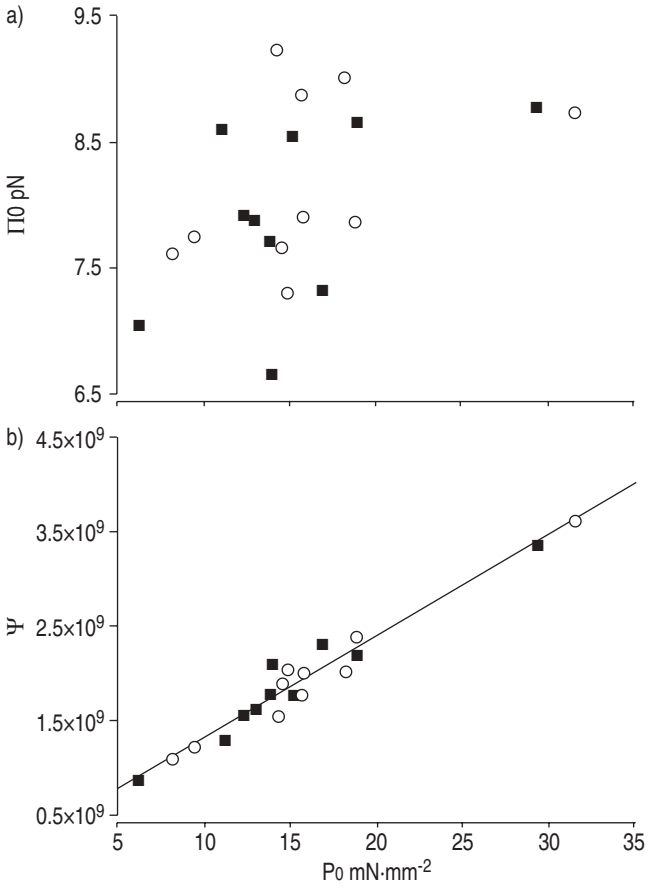

Fig. 6. – Relationships a) between peak isometric tension of muscle strips (P_0) and the unitary force per single crossbridge (Π_0), and b) between P_0 and the number of crossbridges at peak active tension ($\Psi \times 10^9$) in Fisher (○) and Lewis (■) rats. Ψ=0.107 P_0+0.247. r^2=0.951, p<0.0001.

Validation of the animal models

Both Fisher and Lewis are anatomically well-characterised strains of inbred rats [33]. When compared with Lewis, Fisher rats are known to exhibit higher airway responsiveness to various inhaled contractile agonists, such as methacholine [17] or 5-hydroxytryptamine [18, 19]. *In vivo*, this relative AHR is manifested by a shift in the dose/response curve to the aerosolised agonist in both spontaneously breathing [17–19] and mechanically ventilated animals [20]. In the present study,

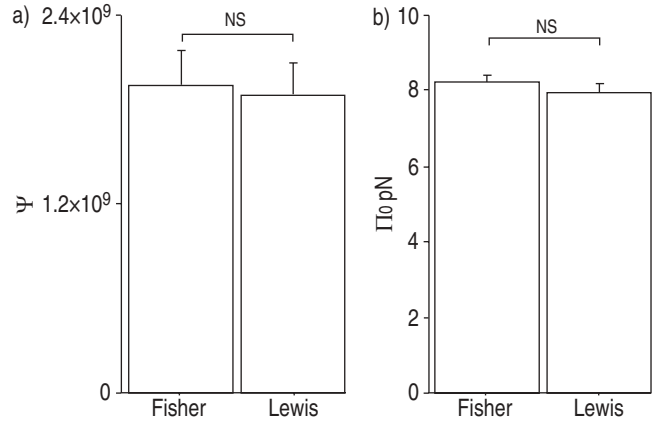

Fig. 5. – Mean±SEM a) calculated total number of myosin crossbridges at peak active tension ($\Psi \times 10^9$) and b) unitary force per crossbridge at peak active tension (Π_0) in Fisher (n=10) and Lewis (n=10) rats. NS: nonsignificant.

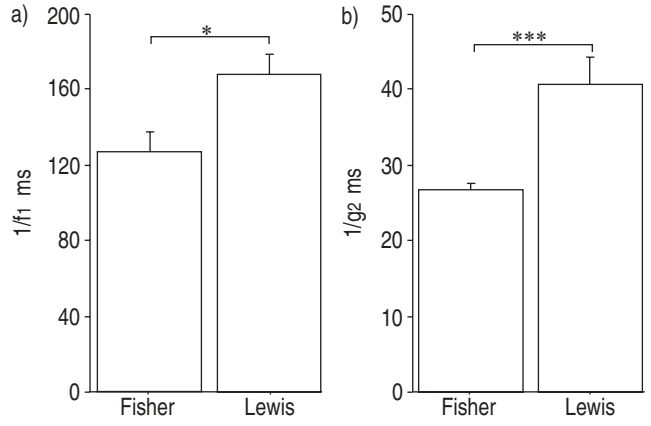

Fig. 7. – Mean±SEM calculated duration of a) crossbridge attachment ($1/f_1$) and b) crossbridge detachment ($1/g_2$) in Fisher (n=10) and Lewis (n=10) rats. *: p<0.05; ***: p<0.001.

in vivo airway responsiveness was not measured in either rat strain. It cannot be excluded therefore that minor differences in airway responsiveness could occur between the rats used in this study and data from the literature. *In vitro*, the ASM of these two rat strains exhibits marked differences; while isolated TSM develops similar isometric force at baseline in both strains [17], the TSM of Fisher rats has been shown to be more responsive to cumulative concentrations of carbachol [34] or serotonin [35] than the Lewis strain. Lung explants have recently been used to show that this innate relative hyperresponsiveness of the Fisher strain was not restricted to the trachea but extended throughout the airway tree [19, 36]. These studies also provided evidence that Fisher rat airways could exhibit a greater capacity for airway narrowing than Lewis. Taken together, these studies support the hypothesis that the relative nonspecific AHR found in the Fisher strain could be related to differences in the intrinsic contractile properties of the ASM [19].

Mechanical contractile properties of tracheal smooth muscle

To the best of the authors' knowledge, no data are available concerning the isotonic contractile properties of isolated TSM of the Fisher and the Lewis strains. The first aim of the present study therefore was to characterise the contractile properties of isolated TSM in both strains, with particular attention paid to isotonic parameters. V_{max} was found to be higher in Fisher than in Lewis rats (fig. 2), as were ΔL and $V_{c,max}$ (fig. 3). These results corroborate previous findings from sensitised dogs [11, 12], guinea-pigs [13], mice [14] and human bronchi [10], which all demonstrated that isolated ASM of sensitised tissue is able to shorten more and faster than ASM of controls. The results could also explain, at least in part, the previous findings reported in lung explants from Fisher and Lewis rats [19, 36].

In ASM, two methods are usually used to elicit the force/velocity relationship; conventional afterloaded isotonic contractions or quick releases applied 2 s after the onset of isometric contractions. Since force/velocity characteristics were first described in canine TSM by STEPHENS *et al.* [37], the best way of eliciting the force/velocity relationship has been a subject of discussion. In a preliminary study, the V_{max} elicited with the afterloaded technique did not differ from the one measured with the quick-release technique [38] in both rat strains. It was also found that experimental data were accurately fitted by a hyperbolic curve, with no obvious deviation of velocities at high load, contrary to results previously reported in dogs [39]. The force/velocity relationship has never been studied in the ASM of rats. Interspecies differences may explain, at least in part, the differences observed between the present data and previous reports in canine TSM. As a hyperbola accurately fitted the current experimental data, the modified equation described by WANG *et al.* [39] was not used. Using the classic HILL [24] equation, parameter b of the equation was higher in Fisher than in Lewis rats, whereas parameter a did not differ between strains (table 1). This result was in agreement with the higher shortening capacity and velocity in Fisher compared with Lewis rats. The G curvature was also found to be similar in both strains (table 1). Similar results have been reported in sensitised canine TSM when compared with controls [11]. In striated muscles, the curvature of the force/velocity relationship has been found to be linked to the myothermal economy of force generation: the more curved Hill's hyperbola (*i.e.* the higher G), the greater the economy of force generation [30, 40]. Assuming that the fundamental properties of myosin CB do not strikingly differ between smooth and striated muscles [26], the present results suggest similar energetic cost of force generation in Fisher and Lewis TSM.

In this study, there were no strain differences in the P_0 developed by isolated electrically stimulated TSM, although F_0 was higher in Fisher than in Lewis rats (fig. 2). In mechanical studies, it is usual to report the results of isometric tension rather than isometric force, as differences in cross-sectional area may interfere with results of force. This was clearly the case in this study. These results are in agreement with those reported previously in the same strains [17] and in animal models of nongenetically determined AHR [10–14].

Myosin crossbridge number, force and kinetics

It has been suggested that the ultimate defect in AHR may be at the muscle cell level itself [14]. If so, it should concern structures, mechanisms or pathways involved in or resulting in higher capacity and velocity of muscle shortening. Several approaches have been used to investigate how myosin molecular motors work. Studies using *in vitro* motility assays [41] and high-resolution single-molecule experiments, such as the optical tweezers technique [42], have provided insights into interactions of elementary contractile proteins. Mathematical models of muscle mechanics provide an informative system for estimating the number, unitary force and kinetics of myosin CB in living muscle [26, 43, 44]. HUXLEY's [26] formalism has been used in many mechanical, as well as biochemical muscle experiments, and can contribute to better understanding of CB interactions [32]. The use of Huxley's equations has been applied to nonsarcomeric muscles, such as smooth muscles, allowing a calculation of CB number, unitary force and kinetics from experimental mechanical data [27]. This has been validated in ASM from several species, including the rat [27]. The reasons for applying Huxley's model in the present study were the following: 1) Huxley's model not only accounts for many macroscopic properties of muscle (force, velocity and heat production), but also relates these properties to its structural and biochemical properties; 2) according to Huxley's model, force and shortening in muscle are generated by cyclic interactions of the myosin heads with specific sites on the thin filaments, with ATP hydrolysis providing the energy; 3) by using mechanical parameters (velocity, length, force) at the level of the entire muscle and at various load levels, Huxley's theory infers the kinetics and number of CB. Thus, the use of Huxley's formalism seemed to be an attractive way to test the hypothesis that inherited, genetically determined mechanical differences could be attributed to differences in CB interactions.

Beside the power stroke, two important steps occur during the CB cycle, *i.e.* the attachment and detachment of the myosin head from actin (fig. 1). Attachment of myosin to actin occurs after ATP hydrolysis [45]. Myosin rapidly dissociates from actin after ADP release. Thereafter, one molecule of ATP binds to the nucleotide site of the myosin head (ATP-binding pocket). In this study, the attachment step was found to be shorter in Fisher than in Lewis rats (fig. 7), and the detachment step was markedly shorter in Fisher than in Lewis rats (fig. 7). A shorter detachment step could account, at least in part, for increased velocity of shortening at the muscle level. In fact, according to Huxley's CB model [26], V_{max} is proportional to the maximum value of g_2; the higher V_{max}, the higher g_2, thus the lower $1/g_2$, *i.e.* the shorter the detachment step. Therefore, the detachment step is a crucial step in the determination of maximum shortening

velocity in ASM. 1/g2, rather than tc, would thus strongly influence the shortening capacity of the whole muscle. Further studies are needed to investigate which structural, biochemical or mechanical factors influence g2 and, to a lesser extent, f1 in the Fisher strain. Potential candidates are as follows: 1) differences in the three-dimensional configuration of the ATP-binding pocket of the myosin head, or the presence of a seven amino acid insert near the ATP-binding pocket [42, 46], or differences in the configuration of the actin-binding site; 2) higher expression of the smooth muscle-B isoform of the myosin heavy chain in Fisher trachea (the presence of this isoform has recently been reported in TSM of adult Fisher rats) [47]; 3) differences in the 20 kD regulatory light chains of myosin; 4) differences in the structure, content or activity of myosin light chain kinase, especially the smMLCK isoform [16]; 5) structural or functional differences in the calcium/calmodulin complex; and 6) differences in the activity of the Rho-associated kinase that can directly phosphorylate the 20 kD regulatory light chains of myosin independently of calcium [48]. However, it should be mentioned that increased intracellular calcium mobilisation has recently been described in Fisher rats when compared with Lewis rats [19], suggesting that calcium-dependent pathways are at least partly involved in the mechanisms underlying the nonspecific AHR of the Fisher strain.

Using Huxley's equations adapted for smooth muscles [27], no interstrain differences were found between the number, unitary force and mean velocity of myosin CB at peak active tension. Moreover, no relationship was found between Vmax and v0. Therefore, greater velocity of muscle shortening observed in Fisher rats could not be attributed to higher velocity of CB during power stroke. Potential differences in tc were also sought but no such differences were found between Fisher and Lewis rats, indicating that higher velocity of shortening is not necessarily associated with a shorter time cycle.

In conclusion, the isotonic and isometric contractile properties of isolated tracheal smooth muscle of Fisher and Lewis inbred rat strains were analysed. The higher genetically determined spontaneous nonspecific airway hyperresponsiveness of the Fisher rat strain was associated with higher shortening capacity and velocity of tracheal smooth muscle when compared with Lewis rats, with no difference in the ability to produce isometric force. These mechanical differences were not attributed to differences in the number, unitary force or mean velocity of myosin crossbridge during power stroke. In contrast, differences in myosin crossbridge kinetics, *i.e.* shorter duration of crossbridge detachment and attachment in Fisher than in Lewis, may help explain the higher shortening capacity and velocity in Fisher rats. These results highlight the crucial role of the crossbridge itself in the phenomenon of innate greater airway responsiveness of the Fisher rat strain.

Appendix: Calculations

Using HUXLEY's [26] manuscript, the authors first expressed the rate of total energy release ($\dot{E}$) and the isotonic tension (PHux) as a function of velocity (V). Thus, $\dot{E}$ is given as:

$$\dot{E} = \Psi\, e \frac{h}{2\ell} \times \frac{f_1}{f_1+g_1}\left\{g_1 + f_1 \frac{V}{\Phi}\left(1-e^{-\frac{\Phi}{V}}\right)\right\} \quad (8)$$

The minimum rate of total energy release ($\dot{E}_o$) occurs under isometric conditions (V=0 in equation 8), is equal to the product of a×b [24, 26] and is given by:

$$\dot{E}_o = ab = \Psi e \frac{h}{2\ell} \times \frac{f_1 g_1}{f_1+g_1} \quad (9)$$

It can be deduced that:

$$\Psi = \dot{E}_o/(ek_{cat}) \quad (10)$$

The isotonic tension PHux is given by equation 11 [26]:

$$P_{Hux} = \frac{\Psi w}{\ell} \times \frac{f_1}{f_1+g_1}\left[1 - \frac{V}{\Phi}\left(1-e^{\frac{-\Phi}{V}}\right)\left(1+\frac{1}{2}\left(\frac{f_1+g_1}{g_2}\right)^2 \frac{V}{\Phi}\right)\right] \quad (11)$$

PHux,max is reached for V=0 and is assumed to be equal to total isometric tension (P0), which was experimentally determined. The mean unitary force per CB in isometric conditions is:

$$\Pi_0 = P_{Hux,max}/\Psi = \frac{w}{\ell}\frac{f_1}{f_1+g_1} \quad (4)$$

Calculation of peak value of detachment rate constant (g2)

As Φ=(f1+g1)h/2, Φ=b, G=g2/(f1+g1) [26] and Vmax=Gb, it is deduced that:

$$g_2 = \frac{2V_{max}}{h} \quad (2)$$

Calculation of detachment rate constant (g1)

From equations 9 (with $\dot{E}_o = ab$) and 11 in isometric conditions (with V=0 and PHux,max=Ga), it was deduced that:

$$\frac{f_1 g_1}{f_1+g_1} = \frac{2\ell ab}{eh\Psi} = \frac{2\ell Ga}{2w\Psi} g_1 \quad (12)$$

Thus,

$$g_1 = \frac{2wb}{ehG} \quad (1)$$

Calculation of peak value of attachment rate constant (f1)

$\dot{E}$ was linearised as a function of PHux.

Let $A = \frac{V}{\Phi}\left(1-e^{\frac{\Phi}{V}}\right)$ and $B = \frac{f_1}{2\ell(f_1+g_1)}$

By replacing A and B in equations 8 and 11, equation 8 becomes:

$$\frac{E}{eh\Psi B} = g_1 + f_1 A \quad (13)$$

Equation 11 becomes:

$$\frac{P_{Hux}}{2w\Psi B} = 1 - A\left(1+\frac{1}{2}\times\frac{d^2V}{\Phi}\right) \quad (14)$$

where d=1/G.

From equation 13, it was deduced that:

$$A = \frac{E}{\Psi ehBf_1} - \frac{g_1}{f_1}$$

From equation 14, it was deduced that:

$$A = \frac{(2w\Psi B - P_{hux})(2\Phi)}{(2w\Psi B)(2\Phi + d^2V)}$$

From equations 13 and 14, it was deduced that:

$$\overset{0}{E} = \frac{2\Phi(eh\Psi Bf_1)}{2\Phi + Vd^2} + g_1(eh\Psi B) - \frac{eh\Phi f_1}{w(2\Phi + Vd^2)} P_{Hux} \quad (15)$$

From equation 15 and near isometric conditions, where V can be neglected ($V \approx 0$), $\overset{0}{E}$ can be linearised as a function of P_{Hux} as follows:

$$\overset{0}{E} = \frac{\Psi ehf_1}{2\ell} - \frac{ehf_1}{2w} P_{Hux} \quad (16)$$

The slope of this relationship between $\overset{0}{E}$ and P_{Hux} has been shown to be equal to b [26, 27], then, $\frac{ehf_1}{2w} = b$ so that:

$$f_1 = \frac{2wb}{eh} \quad (17)$$

From equations 1 and 17 it was deduced that:

$$\frac{2w}{eh} = \frac{g_1 G}{b} = \frac{f_1}{b}. \text{ Thus, } f_1 = Gg_1 \quad (18)$$

As $G=g_2/(f_1+g_1)$ [26] and $f_1=Gg_1$, by solving the quadratic equation $f_1^2+g_1f_1-g_1g_2=0$, f_1 as a function of g_1 and g_2 was obtained:

$$f_1 = \frac{-g_1 + \sqrt{g_1^2 + 4g_1g_2}}{2} \quad (3)$$

References

1. National Heart, Lung and Blood Institute. Global initiative for asthma. Global strategy for asthma management and prevention. Publication no. 95-3659. Bethesda, National Heart, Lung and Blood Institute, 1995; pp. 69–117.
2. American Thoracic Society. Update: future directions for research on diseases of the lung. *Am J Respir Crit Care Med* 1998; 158: 320–334.
3. Brusasco V, Crimi E, Pellegrino R. Airway responsiveness in asthma: not just a matter of airway inflammation. *Thorax* 1998; 53: 992–998.
4. Heard BE, Hossain S. Hyperplasia of bronchial muscle in asthma. *J Pathol* 1973; 110: 319–331.
5. Carroll N, Elliot J, Morton A, James A. The structure of large and small airways in nonfatal and fatal asthma. *Am Rev Respir Dis* 1993; 147: 405–410.
6. Ebina M, Takahashi T, Chiba T, Motomiya M. Cellular hypertrophy and hyperplasia of airway smooth muscles underlying bronchial asthma. A 3-D morphometric study. *Am Rev Respir Dis* 1993; 148: 720–726.
7. Eidelman DH, Di Maria GU, Bellofiore S, Wang NS, Guttmann RD, Martin JG. Strain-related differences in airway smooth muscle and airway responsiveness in the rat. *Am Rev Respir Dis* 1991; 144: 792–796.
8. Thomson RJ, Bramley AM, Schellenberg RR. Airway muscle stereology: implications for increased shortening in asthma. *Am J Respir Crit Care Med* 1996; 154: 749–757.
9. Bramley AM, Thomson RJ, Roberts CR, Schellenberg RR. Hypothesis: excessive bronchoconstriction in asthma is due to decreased airway elastance. *Eur Respir J* 1994; 7: 337–341.
10. Mitchell RW, Rühlmann E, Magnussen H, Leff AR, Rabe KF. Passive sensitization of human bronchi augments smooth muscle shortening velocity and capacity. *Am J Physiol Lung Cell Mol Physiol* 1994; 267: L218–L222.
11. Antonissen LA, Mitchell RW, Kroeger EA, Kepron W, Tse KS, Stephens NL. Mechanical alterations of airway smooth muscle in a canine asthmatic model. *J Appl Physiol* 1979; 46: 681–687.
12. Jiang H, Rao K, Halayko AJ, Kepron W, Stephens NL. Bronchial smooth muscle mechanics of a canine model of allergic airway hyperresponsiveness. *J Appl Physiol* 1992; 72: 39–45.
13. Mitchell RW, Ndukwu IM, Arbetter K, Solway J, Leff AR. Effect of airway inflammation on smooth muscle shortening and contractility in guinea pig trachealis. *Am J Physiol Lung Cell Mol Physiol* 1993; 265: L549–L554.
14. Fan T, Yang M, Halayko A, Mohapatra SS, Stephens NL. Airway responsiveness in two inbred strains of mouse disparate in IgE and IL-4 production. *Am J Respir Cell Mol Biol* 1997; 17: 156–163.
15. Stephens NL, Jiang H. Basic physiology of airway smooth muscle. *In*: Busse WW, Holgate ST, eds. Asthma and Rhinitis. Boston, Blackwell Scientific Publications, 1995; pp. 1087–1115.
16. Ammit AJ, Armour CL, Black JL. Smooth-muscle myosin light-chain kinase content is increased in human sensitized airways. *Am J Respir Crit Care Med* 2000; 161: 257–263.
17. Di Maria GU, Martin JG, Bellofiore S, Mistretta A. Relationship between *in vivo* airway reactivity and *in vitro* responsiveness of tracheal smooth muscle in inbred rats. *Respiration* 1988; 54: Suppl. 1, 108–113.
18. Zacour ME, Martin JG. Enhanced growth response of airway smooth muscle in inbred rats with airway responsiveness. *Am J Respir Cell Mol Biol* 1996; 15: 590–599.
19. Tao FC, Tolloczko B, Eidelman DH, Martin JG. Enhanced Ca^{2+} mobilization in airway smooth muscle contributes to airway hyperresponsiveness in an inbred strain of rat. *Am J Respir Crit Care Med* 1999; 160: 446–453.
20. Dandurand RJ, Xu LJ, Martin JG, Eidelman DH. Airway-parenchymal interdependence and bronchial responsiveness in two highly inbred rat strains. *J Appl Physiol* 1993; 74: 538–544.
21. Bard M, Salmeron S, Coirault C, Blanc F-X, Lecarpentier Y. Effects of initial length on intrinsic tone in guinea-pig tracheal smooth muscle. *Am J Physiol Lung Cell Mol Physiol* 1998; 275: L1026–L1030.
22. Blanc F-X, Salmeron S, Coirault C, *et al.* Effects of load and tone on the mechanics of isolated human bronchial smooth muscle. *J Appl Physiol* 1999; 86: 488–495.
23. Brutsaert DL, Claes VA, Sonnenblick EH. Velocity of shortening of unloaded heart muscle and the length-tension relation. *Circ Res* 1971; 29: 36–75.
24. Hill AV. The heat of shortening and the dynamic constants of muscle. *Proc R Soc Lond Biol Sci* 1938; 126: 136–195.
25. Stephens NL, Halayko A, Jiang H. Normalization of contractile parameters in canine airway smooth muscle: morphological and biochemical. *Can J Physiol Pharmacol* 1992; 70: 635–644.
26. Huxley AF. Muscle structure and theories of contraction. *Progr Biophys Chem* 1957; 7: 255–318.
27. Lecarpentier Y, Blanc F-X, Salmeron S, Pourny JC, Chemla D, Coirault C. Myosin cross-bridge kinetics in airway smooth muscle: a comparative study of humans, rats and rabbits. *Am J Physiol Lung Cell Mol Physiol* 2002; 282: L83–L90.
28. Rayment I, Rypniewski WR, Schmidt-Bäse K, *et al.* Three-dimensional structure of myosin subfragment-1: a molecular motor. *Science* 1993; 261: 50–58.
29. Dominguez R, Freyzon Y, Trybus KM, Cohen C. Crystal structure of a vertebrate smooth muscle myosin motor domain and its complex with the essential light chain: visualization of the pre-power stroke state. *Cell* 1998; 94: 559–571.
30. Woledge RC, Curtin NA, Homsher E. Energetic aspects of muscle contraction. *Mon Physiol Soc* 1985; 41: 27–117.
31. Sheterline P, Clayton J, Sparrow JC, eds. Actins. *In*: Protein Profile. 3rd edn. London, Academic Press, 1996; pp. 1–76.
32. Lecarpentier Y, Chemla D, Blanc F-X, *et al.* Mechanics, energetics, and crossbridge kinetics of rabbit diaphragm during congestive heart failure. *FASEB J* 1998; 12: 981–989.
33. Riesenfeld A. Constitution and body proportions in different strains of rats. *Acta Anat* 1976; 94: 169–183.

34. Jia Y, Xu L, Heisler S, Martin JG. Airways of a hyperresponsive rat strain show decreased relaxant responses to sodium nitroprusside. *Am J Physiol Lung Cell Mol Physiol* 1995; 269: L85–L91.
35. Florio C, Styhler A, Heisler S, Martin JG. Mechanical responses of tracheal tissue *in vitro*: dependance on the tissue preparation employed and relationship to smooth muscle content. *Pulm Pharmacol* 1996; 9: 157–166.
36. Wang CG, Almirall JJ, Dolman CS, Dandurand RJ, Eidelman DH. *In vitro* bronchial responsiveness in two highly inbred rat strains. *J Appl Physiol* 1997; 82: 1445–1452.
37. Stephens NL, Kroeger E, Mehta JA. Force-velocity characteristics of respiratory airway smooth muscle. *J Appl Physiol* 1969; 26: 685–692.
38. Blanc F-X, Salmeron S, Bard M, Coirault C, Lecarpentier Y. Force-velocity curves in isolated tracheal smooth muscle: afterloaded *versus* load clamp method. *Am J Respir Crit Care Med* 1999; 159: A395.
39. Wang J, Jiang H, Stephens NL. A modified force-velocity equation for smooth muscle contraction. *J Appl Physiol* 1994; 76: 253–258.
40. Coirault C, Chemla D, Péry-Man N, Suard I, Lecarpentier Y. Effects of fatigue on force-velocity relation of diaphragm. Energetic implications. *Am J Respir Crit Care Med* 1995; 151: 123–128.
41. Umemoto S, Sellers RJ. Characterization of *in vitro* motility assays using smooth muscle and cytoplasmic myosins. *J Biol Chem* 1990; 265: 14864–14869.
42. Lauzon AM, Tyska MJ, Rovner AS, Freyzon Y, Warshaw DM, Trybus K. A 7-amino-acid insert in the heavy chain nucleotide binding loop alters the kinetic of smooth muscle myosin in the laser trap. *J Muscle Res Cell Motil* 1998; 19: 825–837.
43. Hai CM, Murphy RA. Regulation of shortening velocity by cross-bridge phosphorylation in smooth muscle. *Am J Physiol Cell Physiol* 1988; 255: C86–C94.
44. Fredberg JJ, Inouye DS, Mijailovich SM, Butler JP. Perturbed equilibrium of myosin binding in airway smooth muscle and its implications in bronchospasm. *Am J Respir Crit Care Med* 1999; 159: 959–967.
45. Lymn RW, Taylor EW. Mechanism of ATP hydrolysis by actomyosin. *Biochemistry* 1971; 10: 4617–4624.
46. Lauzon AM, Azoulay E, Maghni K. Smooth muscle myosin heavy chain isoform expression in airway hyperresponsiveness. *Am J Respir Crit Care Med* 2001; 163: A539.
47. Low RB, Mitchell J, Woodcock-Mitchell J, Rovner AS, White SL. Smooth-muscle myosin heavy-chain SM-B isoform expression in developing and adult rat lung. *Am J Respir Cell Mol Biol* 1999; 20: 651–657.
48. Kureishi Y, Kobayashi S, Amano M, *et al.* Rho-associated kinase directly induces smooth muscle contraction through myosin light chain phosphorylation. *J Biol Chem* 1997; 272: 12257–12260.